JOURNAL OF GEOPHYSICAL RESEARCH, VOL. 96, NO. C7, PAGES 12,755–12,771, JULY 15, 1991

Effects of the Gulf Stream on Ocean Waves

L. H. HOLTHUIJSEN AND H. L. TOLMAN[1]

Delft University of Technology, Department of Civil Engineering, Delft, Netherlands

In the present study a third-generation numerical wave model is used to study effects of a straight Gulf Stream and a Gulf Stream ring on ocean waves in swell and storm conditions. The model accounts for all relevant processes of propagation, generation, and dissipation of the waves (including current effects) without imposing a priori restraints on the spectral development of the waves. The dominating mechanism affecting the waves appears to be current-induced refraction even though the short-crestedness of the incoming waves tends to mask its effects (also in swell conditions). Depending on wind and wave conditions, refraction may trap locally generated waves in the straight Gulf Stream or it may reflect wave energy back to the open ocean. In the Gulf Stream ring, refraction induces a considerable variation in significant wave height and short-crestedness, but it hardly affects the mean wave direction. In storm conditions the processes of generation and dissipation are considerably enhanced in countercurrent situations and reduced following-current situations.

1. INTRODUCTION

Observations from ships, aircraft, and spacecraft show that ocean waves approaching the east coast of the United States are affected by the Gulf Stream. The currents tend to create a confused sea state, often with waves that are higher than the incoming waves [e.g., *Fuglister*, 1971; *Beal*, 1980; *Hayes*, 1981; *McClain et al.*, 1982; *Meadows et al.*, 1983; *Dobson and Irvine*, 1983; *Tseng*, 1985; *McLeish and Ross*, 1985; *Mapp et al.*,1985; *Liu et al.*, 1989]. Similar observations have been made off the coast of South Africa, Japan, and California [e.g., *Sugimori*, 1973; *Sheres et al.*, 1985; *Irvine*, 1987; *Irvine and Tilley*, 1988]. Several studies have been carried out to model the effects of such shear currents on the propagation of waves. Some of these studies consider both refraction and diffraction [e.g., *McKee*, 1974, 1975, 1977; *Smith*, 1976; *Booij*, 1981; *Smith*, 1983] whereas others (given below) ignore diffraction. In the following we also ignore diffraction as the corresponding effects are dominated by the short-crested, random nature of the waves (at least at the scales considered here). Our study is aimed at including the dynamic interactions between wind, waves, and currents.

The theory of conservative wave-current interactions has been well developed with the work of *Longuet-Higgins and Stewart* [1960, 1961, 1962], *Whitham* [1965], and *Bretherton and Garrett* [1968] (see *Peregrine* [1976] or *Jonsson* [1989] for reviews). It has been applied at scales varying from coastal regions (e.g., rip currents at the beach) to oceanic regions (e.g., the Gulf Stream). Current-induced changes in wave height and direction have thus been calculated in large-scale rings and straight or meandering currents [e.g., *Kenyon*, 1971; *Hayes*, 1980; *Mapp et al.*, 1985; *Tseng*, 1985; *Gutshabash and Lavrenov*, 1986; *Lai and Bales*, 1986; *Mathiesen*, 1987; *Irvine and Tilley*, 1988; *Trulsen et al.*, 1990]. Also, inverse modeling has been suggested and attempted in the sense that shear currents can be estimated from observable changes in wave characteristics [e.g., *Huang et al.*, 1972; *Sheres et al.*, 1985; *McLeish and Ross*, 1985]. The theory of wave-wind interactions has been fairly well established with the work of *Phillips* [1957], *Miles* [1957], and *Hasselmann* [1960, 1974]. Parametrical representations of these theories have been applied extensively, but explicit, nonparametric representations of these theories have been successfully implemented only recently in wave models. This allows the wave spectrum in the model to develop without a priori restraints (third-generation models, e.g., the WAM model of the WAMDI Group [*Hasselmann et al.*, 1988]).

In the present study we use a spectral wave propagation model with all relevant wave-current interactions included, supplemented with a third-generation representation of the wave-wind interactions. With this model we propagate ocean waves across a ring and additionally across an infinitely long and straight Gulf Stream. In the presentation of the results we show the spatial distribution of the waves and the intensity of the physical processes of generation and dissipation, supplemented with spectral information. The currents vary sufficiently slowly in time to allow the assumption of stationary conditions. We use the model in a limited area so that a formulation in terms of Cartesian coordinates rather than spherical coordinates is adequate.

2. THE WAVE MODEL

The wave model which we use is a discrete spectral model for arbitrary bathymetry, wind fields, and current fields. It has been developed recently to investigate wave-current interactions in tidal seas [*Tolman*, 1990*a*, 1991*a*]. As the model has been described in detail by *Tolman* [1989, 1991*b*], we only give a brief review here. The model computes the development of the action density spectrum with the following action balance equation [e.g., *Whitham*, 1965; *Bretherton and Garrett*, 1968; *Hasselmann et al.*, 1973; *Willebrand*, 1975]:

$$\frac{\partial N(\omega, \theta)}{\partial t} + \frac{\partial C_x N(\omega, \theta)}{\partial x} + \frac{\partial C_y N(\omega, \theta)}{\partial y} + \frac{\partial C_\omega N(\omega, \theta)}{\partial \omega} + \frac{\partial C_\theta N(\omega, \theta)}{\partial \theta} = \frac{S(\omega, \theta)}{\sigma} \quad (1)$$

[1]Now at Laboratory for Atmospheres, NASA Goddard Space Flight Center, Greenbelt, Maryland.

Paper number 91JC00901.
0148-0227/91/91JC-00901$05.00

where $N(\omega, \theta)$ is the action density of the waves as a function of absolute frequency ω and direction of wave propagation θ (normal to the wave crest) and σ is the relative frequency (as observed in a frame of reference moving with the current). The source term $S(\omega, \theta)/\sigma$ represents all processes of wave generation and dissipation. This formulation in terms of action density is more convenient than a formulation in terms of energy density, which would add radiation-stress terms to the equation (e.g., *Phillips* [1977] or section 4.1, of this paper). Radiation-stress effects are implicit in the above action density balance. We will evaluate them separately on the basis of the computed wave fields.

The left-hand side of (1) represents the local rate of change of the action density (first term), rectilinear propagation in geographic space (second and third terms with C_x and C_y), shifting of the absolute frequency due to time variations in depth and currents (fourth term with C_ω), and refraction (fifth term with C_θ). The propagation speeds in geographic space (C_x and C_y) are the group velocity components in the x and y directions, respectively (current speed included). The propagation speeds C_ω and C_θ are given by [*Christoffersen*, 1982; *Mei*, 1989]:

$$C_\omega = \frac{\partial \sigma}{\partial d}\frac{\partial d}{\partial t} + \mathbf{k} \cdot \frac{\partial \mathbf{U}}{\partial t} \tag{2}$$

$$C_\theta = -\frac{1}{k}\left[\frac{\partial \sigma}{\partial d}\frac{\partial d}{\partial m} + \mathbf{k} \cdot \frac{\partial \mathbf{U}}{\partial m}\right] \tag{3}$$

in which d is depth, $\mathbf{k}$ is the wave number vector, $\mathbf{U}$ is the current velocity vector, and m is a coordinate orthogonal to the wave direction. These propagation speeds fully account for the depth and current effects on propagation within the linear theory of slowly varying surface gravity waves in a plane. The effects of depth-induced variations of C_x and C_y are normally referred to as "shoaling." To include the current-induced variations, we use the term "straining" instead. We consider stationary situations in deep water so that all terms involving finite depth and time derivatives of the current are zero (i.e., no shoaling, no depth refraction, and no shift of absolute frequencies).

The right-hand side of (1) (the net production of wave action) represents all effects of generation and dissipation of the waves. The processes included in the model are wave generation by wind [*Snyder et al.*, 1981], nonlinear resonant wave-wave interactions [*Hasselmann*, 1960; *Phillips*, 1960], whitecapping [*Komen et al.*, 1984] and bottom-induced dissipation [*Madsen et al.*, 1988]. The actual formulations which we use are those of the WAM model [*Hasselmann et al.*, 1988] except for the formulation of the bottom dissipation (but as this has no relevance for the present study, it will be ignored in the following). The model is therefore, like the WAM model, a third-generation wave model in which the wave spectrum develops free of any a priori restraints. All of these processes of generation and dissipation are formulated in a frame of reference moving with the current (implying the use of the relative wind speed). The effects of currents are accounted for by a transformation to a stationary reference frame in each time step of the model (see below). In the swell cases that we consider, the wave steepness is mild and the wind is absent so that generation, whitecapping, and nonlinear wave-wave interactions are also practically absent. Any variation in the wave field is therefore almost entirely due to refraction, straining, and work done by the radiation stresses. The swell cases have therefore been computed with $S(\omega, \theta)/\sigma = 0$ until a stationary situation was achieved. The computations were then continued for 6 hours with $S(\omega, \theta)/\sigma$ fully included to inspect the expected marginal effect (which was confirmed in every case). In the storm cases that we consider, the term $S(\omega, \theta)/\sigma$ has always been fully included.

The numerical schemes that are used in the model to propagate the waves are second-order accurate finite difference schemes on regular, rectangular grids in x, y, ω, and θ space. When occasionally negative wave action is generated in the model (by numerical inaccuracies, related to an occasional sharp gradient in the wave field), the numerical schemes automatically reduce to first-order accuracy to avoid instability. This occurs only occasionally, momentarily, and locally so that the model is predominantly second-order accurate. The numerical computation of the source term $S(\omega, \theta)/\sigma$ in the model (except bottom-induced dissipation) is identical in every respect to that in the WAM model. To account for current influences, it is supplemented at each time step with a transformation from a frame of reference moving with the current to a fixed frame of reference (Jacobian transformation). The method of integration in time of these source terms is a simple Euler method [e.g., *Abbott*, 1979] which is more economical than the semi-implicit method of the WAM model. The results in standard tests are very similar to those of the WAM model, since the same measures are taken as in the WAM model to maintain stability in wave growth [*Tolman*, 1989]. The spatial resolution in the model is $\Delta x = \Delta y = 13.9$ km for the Gulf Stream and 15 km for the ring. The frequency resolution is $\Delta f = 0.1f$ (absolute frequency $f = \omega/2\pi$ from 0.042 to 0.131 Hz in swell cases and from 0.042 to 0.453 Hz in storm cases) and the directional resolution is $\Delta\theta = 15°$ (storm cases) and $\Delta\theta = 7.5°$ (swell cases). The time step in the model is $\Delta t = 7.5$ min. This directional resolution seems to be adequate for most of the wave fields considered. However, in the swell cases the directional spreading of the swell occasionally decreases to less than 10°. This implies that locally the directional resolution of the model is insufficient (even though it is about 4 times as fine as that commonly used for ocean wave models). Some minor spurious energy is consequently diffused from the original energy-carrying directions to adjacent directions (for a review of this problem of numerical diffusion along the circle, see *Neu and Won* [1990]). In the case of swell approaching the Gulf Stream from the NE direction, this diffused energy bifurcates into the direction of the Gulf Stream current, where it remains and accumulates owing to wave trapping (see below). But it remains small and well identified, and we could filter it out from the computational results of this case (it unduly affects higher-order wave parameters such as the short-crestedness). It probably also occurs in the NE storm case in the Gulf Stream, but the effects there are small compared with the effects of wave generation and dissipation.

One consequence of our model being formulated in terms of finite differences on regular, rectangular grids in x, y, ω, and θ space is that we do not obtain wave ray patterns for individual wave components. These would be very instructive (in fact, we will refer to such patterns), but they can also be somewhat misleading. To illustrate this we note that in our model the wave fields vary fairly smoothly (e.g., Figure

9) where wave ray patterns suggest sharp gradients near caustics (the envelope of neighboring crossing wave rays) (Figure 8 and also *Sheres et al.* [1985], *Mathiesen* [1987], *Irvine and Tilley* [1988], and *Liu et al.* [1989]). This considerable difference in estimating refraction effects is also noted elsewhere in the literature [e.g., *Lavrenov and Ryvkin*, 1986; *Holthuijsen et al.*, 1989]. We do not imply that caustics do not occur in random, short-crested waves; rather we imply that their effects are diffused by the random, short-crested character of the waves [e.g., *Dorrestein*, 1960].

In the interpretation of the model results in the straight Gulf Stream, we use analytical results based on the linear wave theory for unidirectional, monochromatic waves (ignoring wave generation and dissipation). To assess refraction-induced variations in wave direction for straight shear currents, we use the following simple relationship [*Johnson*, 1947; *Sheres et al.*, 1985]:

$$\sin(\theta_2) = \sin(\theta_1)\left[1 - \frac{U}{C\sin(\theta_1)}\right]^{-2} \tag{4}$$

where θ is the angle of incidence relative to the normal of the current, U is the current speed, and C is the phase speed of the wave in a frame of reference moving with the current. The indices 1 and 2 refer to regions outside and inside the shear current, respectively. The change in amplitude a_2/a_1 is readily estimated in this stationary situation from the conservation of absolute frequency ω, wave number vector parallel to current, and action flux orthogonal to current. These computations are conventional as far as refraction and radiation stresses are concerned: $(a_2/a_1)_{\text{refraction}} = \{\cos(\theta_1)/\cos(\theta_2)\}^{1/2}$ and $(a_2/a_1)_{\text{rad.stress}} = (k_2/k_1)^{1/2}$, respectively. To compute the straining effects, we use the approximation of *Tolman* [1990*b*, Appendix A]:

$$(a_2/a_1)_{\text{straining}} = \left(1 + \frac{3}{2}\frac{U_p}{C_g}\right)^{1/2} \tag{5}$$

where U_p is the current velocity component in the wave direction and C_g is the propagation velocity of wave energy in a frame of reference moving with the current.

3. Current, Wave, and Wind Conditions

The current fields we use are taken from a 1-week climatological forecast computed for this study by S. Glenn of Harvard University. For this purpose, Glenn used the Harvard Gulf Stream Forecasting Program [*Glenn*, 1987; *Robinson et al.*, 1988] with the Gulf Stream at its climatological location and a warm core ring in a typical location. The currents thus obtained vary sufficiently slowly in time to treat the current field as stationary. We accordingly select a forecasted current field at one moment in time, and we ignore the time derivatives of the currents. This moment we take roughly halfway through the 1-week forecast.

To obtain the infinitely long, straight Gulf Stream, we synthesize a 150-km-wide transverse surface current profile by averaging the surface current profile of the forecasted Gulf Stream over a 250-km-long section (Figure 1). For convenience of discussion, we take the current in this synthesized Gulf Stream to run from south to north (the actual direction is immaterial, as only the relative directions of waves and currents are relevant). The surface current field of the ring is obtained by isolating a 250 km × 250 km area from the forecasted field (Figure 8).

To obtain a well-defined wave situation in the above current situations we take uniform wave boundary conditions at the open-ocean side of the current fields (some distance upwave from the current boundary). To demonstrate a number of effects as clearly as possible, we have chosen two fairly extreme situations: swell (fairly long crested, fairly regular waves; no wind) and a local storm (short-crested, irregular waves; wind speed at 10-m elevation, $U_{10} = 20$ m s^{-1}). The upwave boundary condition in the storm is characterized with a two-dimensional Joint North Sea Wave Project (JONSWAP) spectrum [*Hasselmann et al.*, 1973] of nearly fully developed waves with a $\cos^{2s}[(\theta - \theta_0)/2]$-directional energy distribution. The value of the directional width parameter s is taken from *Hasselmann et al.* [1980]. The swell boundary condition is characterized with a Gaussian-shaped frequency energy spectrum (standard deviation, σ_f) and a $\cos^{20}(\theta - \theta_0)$-directional energy distribution. Details of the spectral characteristics are given in Table 1. We consider two incoming wave directions relative to the Gulf Stream (swell and storm): 45° from a countercurrent direction (i.e., waves from northeast) and 45° from a following-current direction (i.e. waves from southeast). In the case of the ring the direction of approach is not relevant, as the current field is practically rotationally symmetrical. We therefore consider for the ring only one mean wave direction (from east to west for convenience of the discussion).

For the model computations in and around the ring, we use the full two-dimensional wave model oriented with its x axis along the wind direction. The lateral boundary conditions are taken from the ambient situation which has been computed with a one-dimensional version of the wave model. In this version of the model all lateral gradients affecting propagation in geographic space set at zero (making the ambient wave field effectively infinitely wide). This one-dimensional version of the model is also used for the computations in the straight Gulf Stream with the x axis normal to the current. This effectively makes the Gulf Stream infinitely long. In each situation that we consider the action balance equation is integrated in time until a stationary state is reached. For the ring cases, this is achieved for the integral wave parameters (see below) after twice the propagation time of the peak frequency through the area of the ring. In the straight Gulf Stream it requires 5 times the propagation time through the Gulf Stream owing to trapping of waves which require longer to develop.

4. Results

4.1. *Calculated Quantities*

To quantify the effects of the currents on the wave field, we consider the significant wave height H_s, the mean wave length L_m, the mean wave direction θ_0, and the directional width of the spectrum σ_θ (it will be used as a measure of short-crestedness) as defined next.

$$H_s = 4\sqrt{\sigma_\eta} \tag{6}$$

$$L_m = \frac{1}{\sigma_\eta^2}\int\int \frac{2\pi}{k} N(\omega, \theta)\, d\omega\, d\theta \tag{7}$$

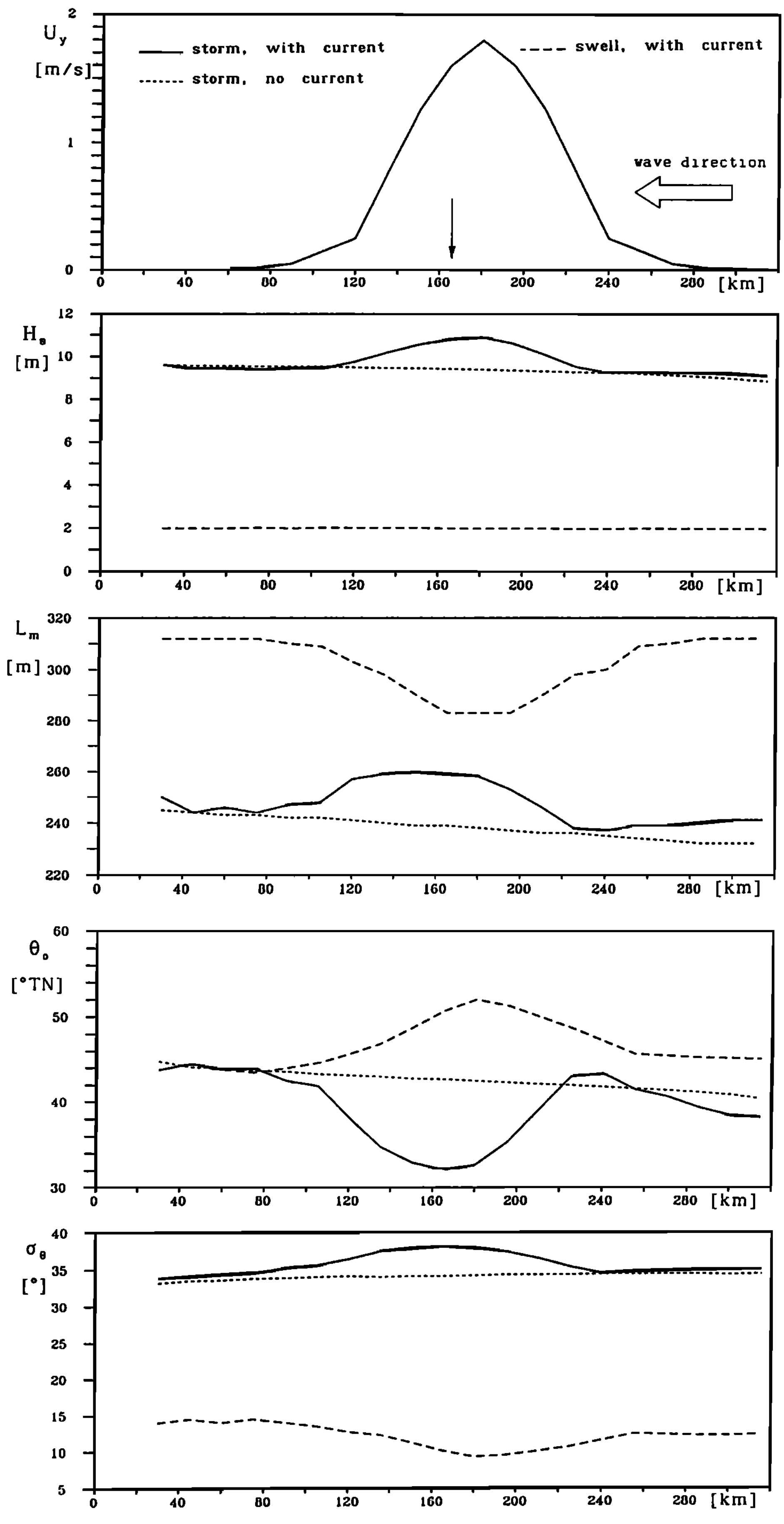

Fig. 1. Profiles in the straight Gulf Stream for waves from a countercurrent direction (NE): current speed U_y, significant wave height H_s, mean wave length L_m, and direction θ_0 (nautical convention), and directional spreading σ_θ. The vertical arrow indicates the location of the spectrum of Figure 2.

TABLE 1. Spectral Characteristics of the Wave Boundary Conditions in the Storm and Swell Cases

Spectral Characteristics	Storm	Swell
Peak frequency		
f_{peak}, Hz	0.073	0.071
Peak width		
σ_a	0.07	...
σ_b	0.09	...
σ_f, Hz	...	0.007
Peak enhancement		
γ	1.49	...
Significant wave height		
H_s, m	8.10	1.99
Directional width		
σ_θ, deg	34.5	12.4

The parameters σ_a, σ_b, and γ are shape parameters of the spectral peak [see *Hasselmann et al.*, 1973].

$$\theta_0 = \text{arctant}\left(\frac{b_1}{a_1}\right) \tag{8}$$

$$\sigma_\theta = \sqrt{2(1 - m_1)} \tag{9}$$

where σ_η is the rms surface elevation, a_1 and b_1 are the first Fourier components of the frequency-integrated directional variance distribution and m_1 is the first Fourier cos-component of this distribution centred around the mean wave direction (for the directional parameters, see *Kuik et al.* [1988]). To represent the physical processes of wave generation and dissipation, we define the intensity of wind input (T_{in}), dissipation due to whitecapping (T_{ds}), and nonlinear wave-wave interactions (T_{nl}) as,

$$T_{in} = \int\int S_{in}(\omega, \theta)\, d\omega\, d\theta \tag{10}$$

$$T_{ds} = \int\int S_{ds}(\omega, \theta)\, d\omega\, d\theta \tag{11}$$

$$T_{nl} = \int\int |S_{nl}(\omega, \theta)|\, d\omega\, d\theta \tag{12}$$

The integrals for computing the integral wave parameters are taken over the entire frequency range of the model. The source terms are integrated over the range in which they are computed (as in the WAM model from f_{low} = 0.042 Hz to f_{high} = max ($2.5f_{peak}$, f_{PM}) where f_{PM} is the Pierson-Moskowitz frequency, [*Pierson and Moskowitz*, 1964]). Note that the absolute value of $S_{nl}(\omega, \theta)$ is taken in the definition of T_{nl}. The total work done (per unit time) by the radiation stresses Γ is defined as the integral over all radiation stress terms in the energy balance equation (not given here, but readily obtained from the action balance equation [e.g., *Phillips*, 1977]),

$$\Gamma = \sum_i \sum_j \int\int \gamma_{ij}(\omega, \theta) \frac{\partial U_i}{\partial x_j}\, d\omega\, d\theta \tag{13}$$

where $\gamma_{ij}(\omega, \theta)$ is the radiation stress tensor defined as

$$\gamma_{ij}(\omega, \theta) = \left[\frac{k_i k_j}{k^2}\frac{C_g}{C} + \frac{1}{2}\left(\frac{2C_g}{C} - 1\right)\delta_{ij}\right]E(\omega, \theta) \tag{14}$$

where $E(\omega, \theta)$ is the variance density spectrum and δ_{ij} is the Kronecker delta.

4.2. *Results for the Straight Gulf Stream*

The synthesized Gulf Stream considered here is straight, and one would perhaps expect it to act more or less as a plane sheet of optical glass in the geometrical optics approximation. This would imply that waves that do not reflect off the Gulf Stream would return to their original state (amplitude, direction, length) when leaving the Gulf Stream at the downwave side. The following shows that is true in a broad sense in the southeast (SE) cases (following current) but not in the northeast (NE) cases (counter current) in which these simple expectations are upset by locally generated waves.

4.2.1. *Swell from the NE direction.* In the NE swell case the wave field shows rather small variations in the primary wave parameters (Figure 1), which can be well understood as shown by the following analytical inspection.

Refraction in this NE swell case turns all energy-carrying wave components more orthogonal to the current. This turning corresponds to a divergence of wave propagation, which would result in a decrease of the significant wave height in the center of the Gulf Stream. On the other hand, straining and work done by the radiation stresses would increase the significant wave height (due to the increasing countercurrent in the wave direction). The analytical solution for the effects of refraction, straining, and radiation stresses for a long-crested, monochromatic wave of 0.07 Hz from direction 45° (nautical convention) (the peak frequency and mean direction of the swell considered here) shows that these effects would roughly cancel out (in the center of the Gulf Stream, refraction would subtract 6% of the incoming energy, and straining and radiation stresses would add 4.6 and 2.5% respectively), resulting in a nearly constant significant wave height, in agreement with the results shown in Figure 1. Theoretically, a similar competition between refraction on the one hand and straining and radiation stresses on the other occurs for the mean wave direction. Refraction turns the mean wave direction clockwise (analytically estimated at about 6° clockwise near the center of the Gulf Stream for the same long-crested, monochromatic wave as above). On the other hand, straining and radiation stresses would turn the mean wave direction counterclockwise as wave components traveling against the current are more enhanced than other wave components. However, if the directional spreading of the waves is small (as for the present swell), the variation in straining and radiation stresses over the directions is small, and this type of turning hardly occurs. This is indeed the case considering the computational results in which the mean wave direction in the Gulf Stream has turned 6.3° clockwise. The increase in long-crestedness of the swell as it approaches the center of the Gulf Stream (the directional width σ_θ decreases from 12.2° to 9.5°) is similarly caused by refraction as all energy-carrying wave components turn toward the same direction. The mean wave length is primarily affected by straining as shown by the analytical solution of the same long-crested, monochromatic wave as above (maximum 11% decrease as compared with 10% in the model results).

As was indicated in section 2, these results were obtained after filtering out energy that was numerically diffused to directions which are trapped in the Gulf Stream. This diffused energy appeared as a secondary peak in a direction well away from the main peak. After 48 hours of swell propagation through the area the situation was practically stationary and we terminated the computations. At that time the secondary peak near the center of the Gulf Stream (where the maximum diffusion effects occurred) contained 5% of the total wave energy there. It caused the mean wave direction θ_0 there to turn 2.2° counterclockwise and the directional spreading σ_θ to increase by 6.4°. As was noted above, we removed this secondary peak.

4.2.2. *Storm from the NE direction.* In the NE storm case the significant wave height increases across the Gulf Stream from 8.1 m to 9.6 m with an overshoot to 10.9 m at the center of the Gulf Stream (Figure 1). The relative variation in this case is therefore much larger than in the swell case discussed above. Also the variations in the mean wave direction, the mean wave length and the short-crestedness are rather different from those in the swell case (Figure 1): the direction turns counterclockwise instead of clockwise, the mean wave length increases rather than decreases, and the waves grow somewhat more short-crested rather than long-crested. The reversal of these three phenomena compared with the swell case, combined with the overshoot in significant wave height, suggests that some low-frequency wave energy is generated and contained near the center of the Gulf Stream. This is indeed the case. Wave energy from northerly directions is added to the incoming spectrum. It creates a second peak in the spectrum (Figure 2, just downwave from the Gulf Stream center; see Figure 1) or it blends with the original peak (at other locations, not shown here), shifting the mean wave direction northward and increasing the directional spreading. This energy is carried by somewhat lower frequencies than the energy of the original spectrum, slightly increasing the mean wave length. An analytical inspection shows that these waves from northerly directions propagate along undulating wave rays near the center of the Gulf Stream. These trapped wave components cannot penetrate the Gulf Stream from the open ocean; they are locally generated by the wind. The analytically determined directional sector in which waves can be trapped is indicated in the aforementioned spectrum (Figure 2). Trapping of waves in a shear current has been noted in the literature before. *McKee* [1975, 1977], *Gutshabash and Lavrenov* [1986], and *Irvine and Tilley* [1988] have shown such trapping in straight and meandering shear currents. Our computations confirm the possibility of trapping locally generated waves as suggested earlier by *Johnson* [1947], *Kenyon* [1971], and *Trulsen et al.* [1990].

In this NE storm case the processes of generation and dissipation are active, in particular in the area with currents. The effect of the (counter-) currents is to considerably enhance the intensity of these processes near the Gulf Stream center (Figure 3): nearly a doubling of the dissipation and the nonlinear interactions and a 50% higher wind input (compared with the undisturbed, i.e., no-current, situation, also shown in Figure 3). These considerable effects are probably due to a large extent to the trapping of the locally generated wave components. They increase the wave steepness, thereby increasing the nonlinear wave-wave interactions and the whitecapping. The increase in apparent wind speed (due to the countercurrent) may also have some effect. But even without wave trapping an increase in whitecapping may occur as was noted by *Phillips* [1977] and observed by *McClain et al.* [1982]. The work done by the radiation stresses is only a small fraction of the source terms individually (Figure 3), but it is about 15% of the total rate of development (wind input and dissipation combined).

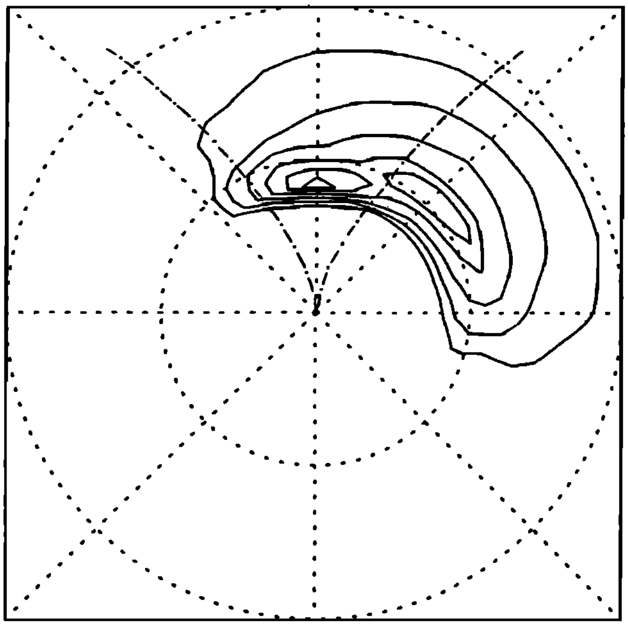

Fig. 2. The two-dimensional variance density spectrum in the straight Gulf Stream at location x = 166.8 km (see Figure 1) for waves in storm conditions from a cross-current direction (NE). The sector in which wave trapping can occur is indicated with dot-dash lines. Contour line values are 0.05, 0.1, 0.2, 0.4, 0.6, and 0.8 times the peak value; the inner circle corresponds to the peak frequency of the one-dimensional (absolute) frequency spectrum and the outer circle to twice the peak frequency. The value of the peak frequency is 0.067 Hz (the sixth model frequency) in this figure and 0.074 Hz (the seventh model frequency) in every other spectral illustration.

4.2.3. *Swell from the SE direction.* If swell enters the Gulf Stream from the SE direction, the variations in the wave field are somewhat larger than in the NE swell case (Figure 4). This larger variation is related to the reflection of some wave energy off the Gulf Stream back to the open ocean (which cannot occur in the counter-current situation described above). This is illustrated here with a spectrum at the upwave side of the Gulf Stream and a spectrum at the downwave side (Figure 5; for locations see Figure 4). These spectra show that at the upwave side about 15% of the incoming wave energy is added to the original spectrum from the SSW direction and that at the downwave side this wave energy is missing from the SSE directional sector. Apparently, wave energy is reflected at wave directions larger than 155°. This agrees well (within the directional resolution of the model $\Delta\theta$ = 7.5°) with the analytically determined angle of reflection of 149° for a 0.07-Hz wave component. The reflected energy travels across the incoming waves, affecting both the mean wave direction and the short-crestedness. It turns the mean wave direction at the open ocean side clockwise (from the undisturbed open ocean value of 135° to 142°) and it makes the waves more short-crested (σ_θ from the undisturbed value of 12.4° to 24.9°). The directional effects at the downwave side (where the reflected energy is missing) are smaller than and opposite to those at the upwave side. The reason of these effects being smaller is that the missing energy is more aligned with the undisturbed spectrum than

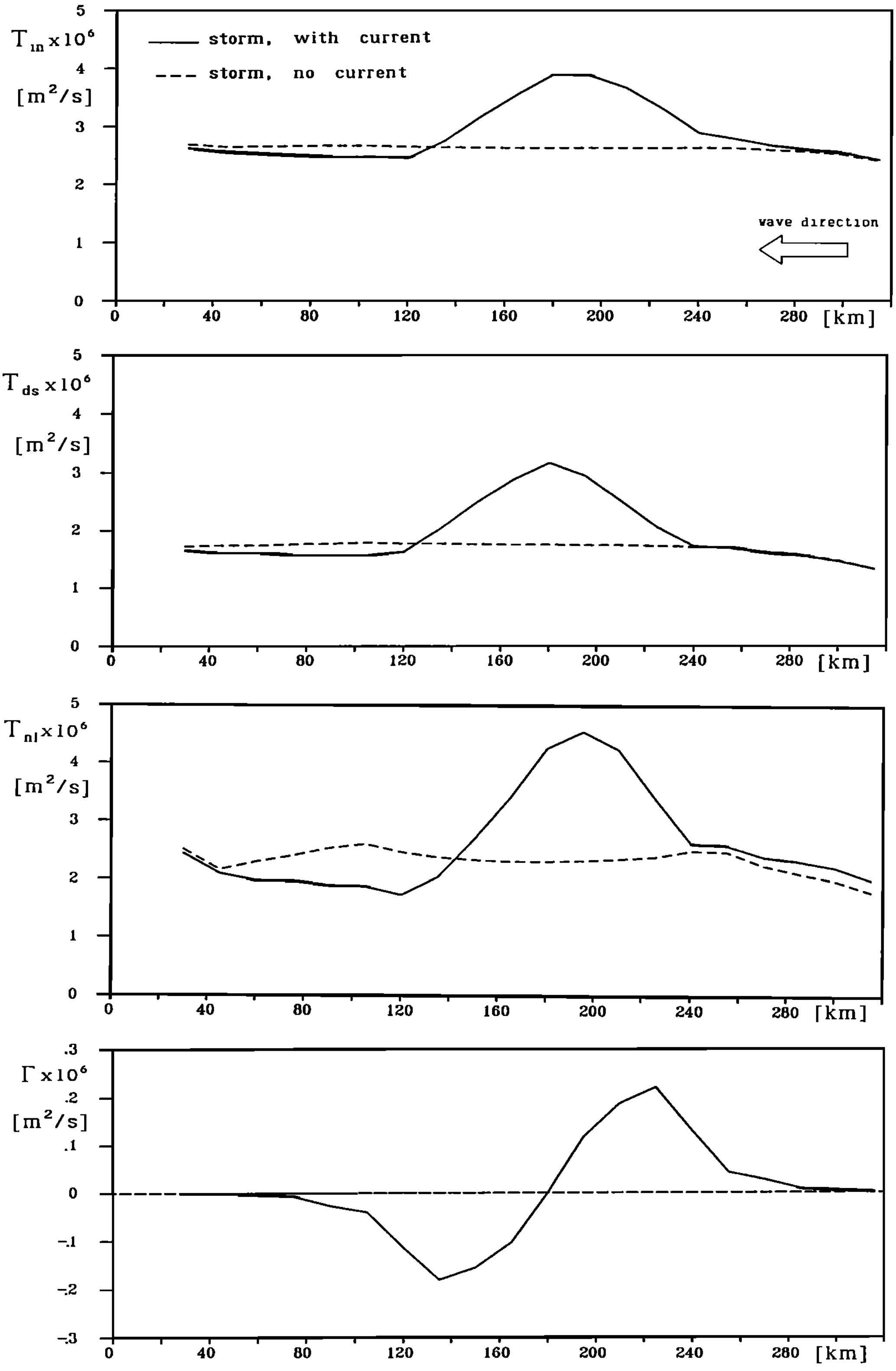

Fig. 3. Profiles in the straight Gulf Stream for storm conditions from a countercurrent direction (NE): wind input T_{in}, dissipation T_{ds}, nonlinear wave-wave interactions T_{nl}, and radiation stress work Γ.

the reflecting energy. Such a reflection in a straight shear current is a well-known phenomenon [e.g., *Kenyon*, 1971; *McKee*, 1974, 1975, 1977; *Smith*, 1976; *Jonsson and Skovgaard*, 1978; *Hayes*, 1980; *Smith*, 1983; *Lai and Bales*, 1986; *Neu and Won*, 1990; *Trulsen et al.*, 1990]. *Irvine* [1987] and *Irvine and Tilley* [1988] show that in a meandering current such reflection may occur as well. The variation in mean wave length in the computations is again in agreement with the analytically determined variation for the above monochromatic, long-crested wave component of 0.07 Hz.

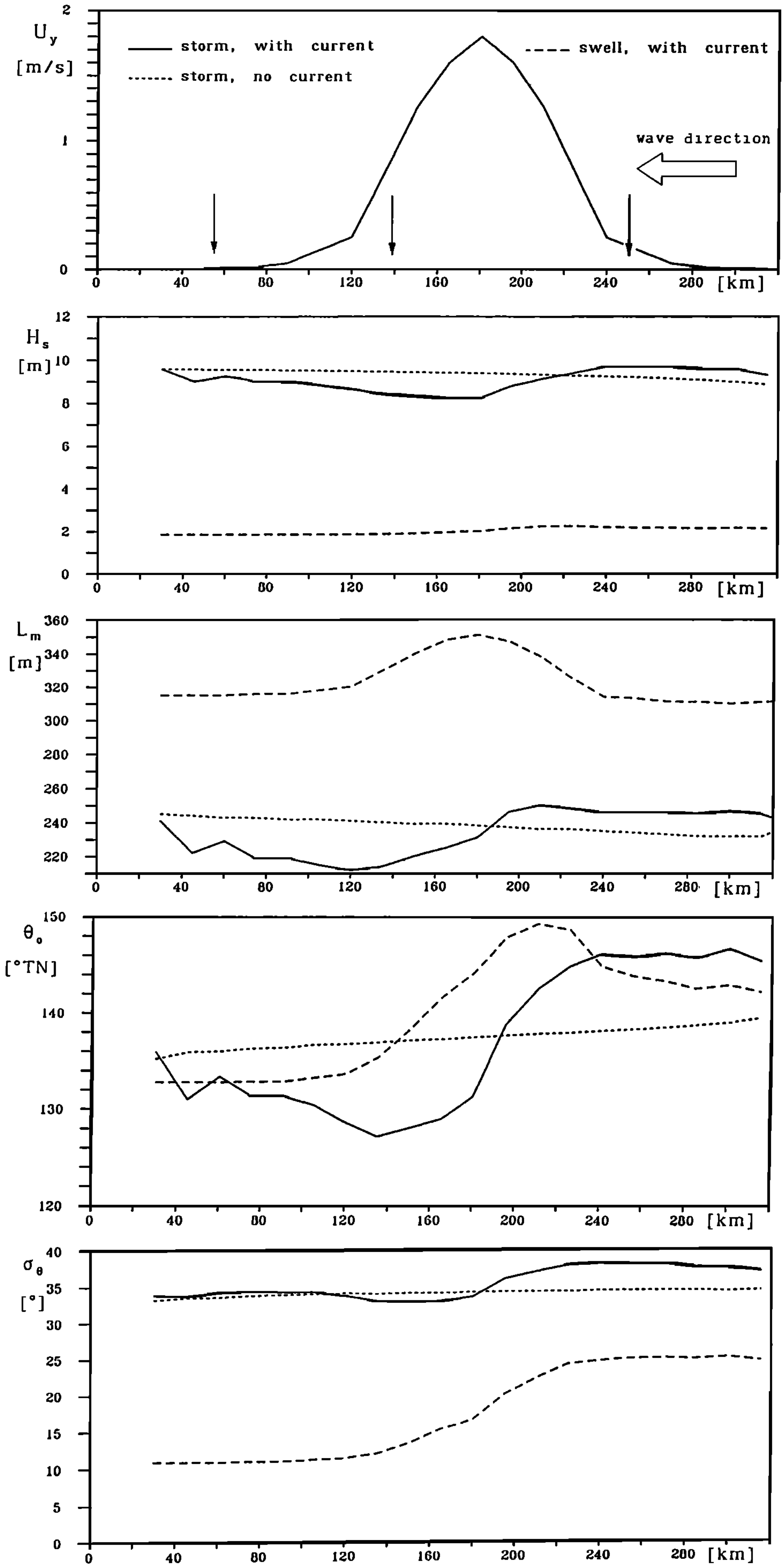

Fig. 4. Profiles in the straight Gulf Stream for waves from the following-current direction (SE): current speed U_y, significant wave height H_s, mean wave length L_m, and direction θ_0 (nautical convention), and directional spreading σ_θ. Vertical arrows indicate locations of the spectra of Figures 5 and 6.

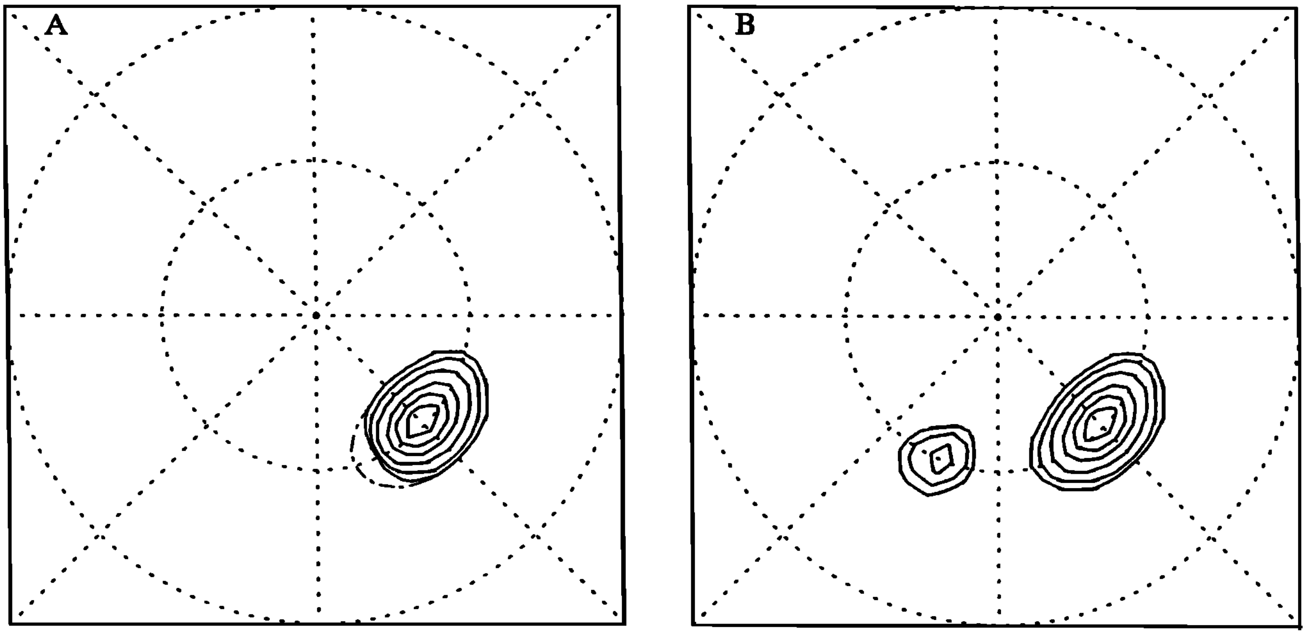

Fig. 5. Two-dimensional spectra in the straight Gulf Stream at locations (*a*) downwave from the Gulf Stream center (x = 55.6 km) and (*b*) upwave from the Gulf Stream center (x = 250.2 km) for swell from a following-current direction (SE). For locations, see Figure 4. For plot legend, see Figure 2. Missing energy is indicated with dot-dash line in Figure 5*a*.

4.2.4. *Storm from the SE direction.* In the case of the SE storm, the pattern of the variations in the wave field are fairly similar to those in the swell case discussed above (Figure 4) and reflection is even more important than in the swell case. This is evident in the relatively large decrease of the computed significant wave height near the center of the Gulf Stream. The spectrum just upwave from the center correspondingly contains energy traveling from southerly and south-southwesterly directions (Figure 6). This reflected energy is obviously missing from the wave field just downwave from the center of the Gulf Stream, although the wind has already generated some high-frequency energy in this sector (Figure 6). It causes the mean wave length to shorten somewhat. Upwave from the Gulf Stream the reflected energy is rapidly dissipated, and the spectrum is only mildly affected.

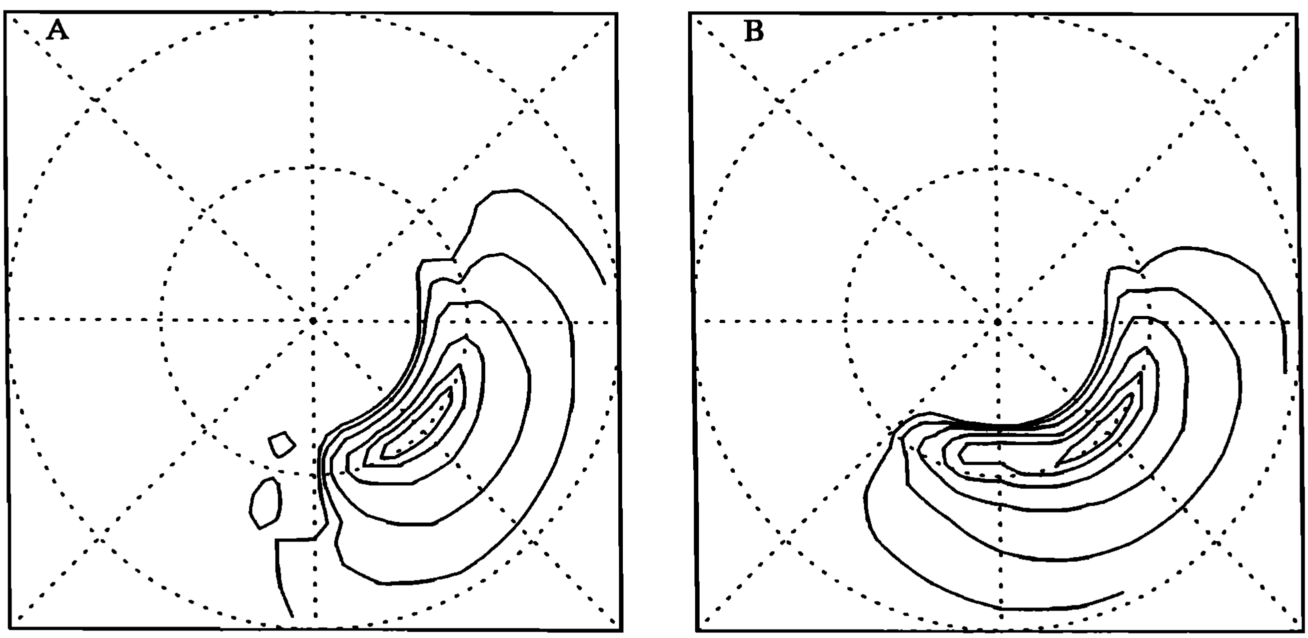

Fig. 6. Two-dimensional spectra in the straight Gulf Stream at locations (*a*) downwave from the Gulf Stream center (x = 139.0 km) and (*b*) upwave from the Gulf Stream center (x = 250.2 km) for storm from a following-current direction (SE). For location, see Figure 4. For plot legend, see Figure 2.

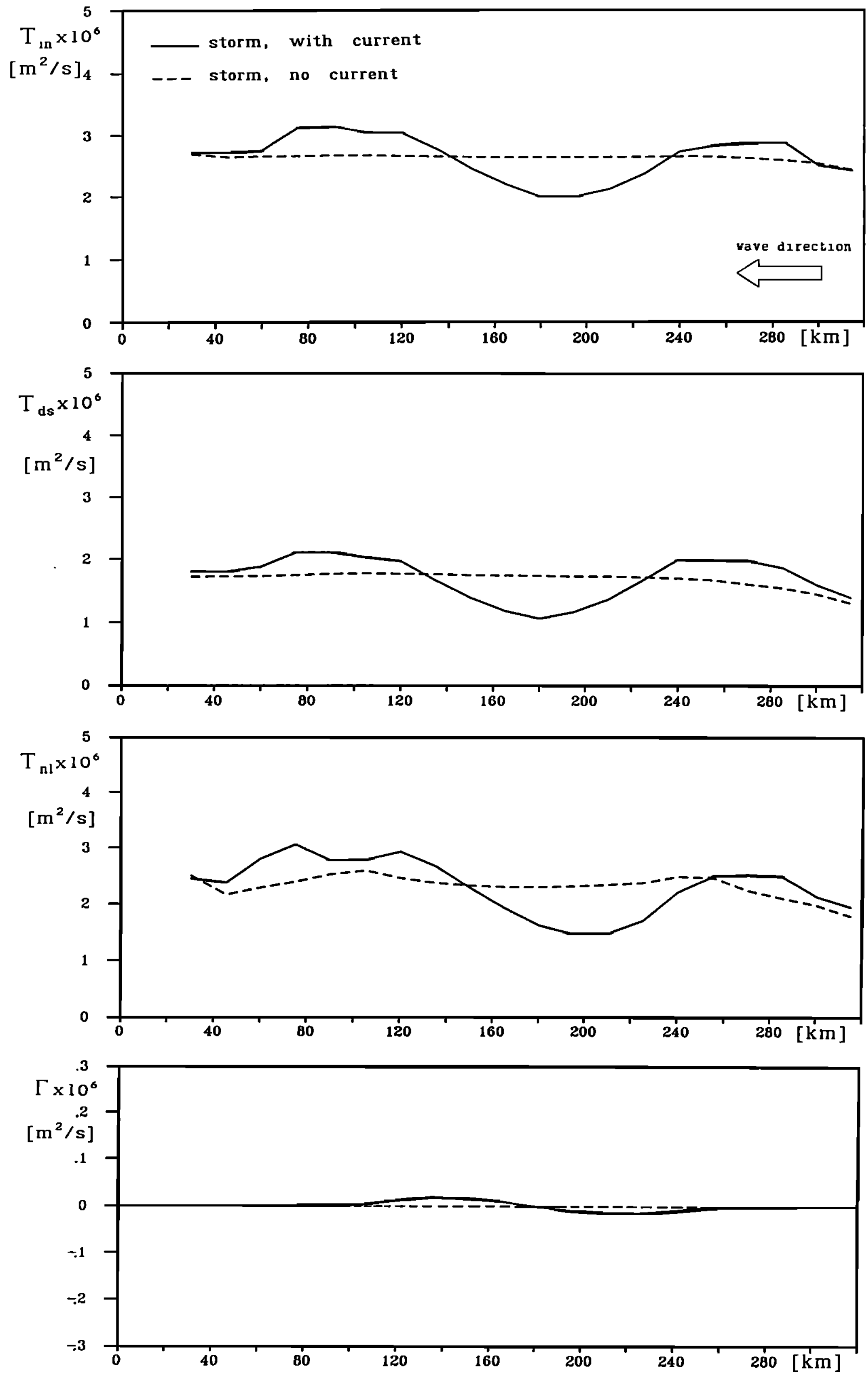

Fig. 7. Profiles in the straight Gulf Stream for storm conditions from a following-current direction (SE): wind input T_{in}, dissipation T_{ds}, nonlinear wave-wave interactions T_{nl}, and radiation stress work Γ.

In contrast to the NE storm, the intensity of all processes of generation and dissipation in this SE storm are reduced in the center of the Gulf Stream (compared with the undisturbed situation) and somewhat enhanced at the boundaries of the Gulf Stream (Figure 7). This is probably due to the current-induced decrease in wave steepness and a reduction of the apparent wind speed.

4.3. *Results for the Gulf Stream Ring*

The following results show that the ring induces larger gradients in the wave field than the straight Gulf Stream does. The reason is the asymmetry of the ring across the wave directions: it contains both following currents and countercurrents, inducing opposite effects within an area with roughly the dimension of the Gulf Stream width. As we indicated in the introduction, we consider only one swell case and one storm case because a variation in incoming wave direction is irrelevant for the nearly rotationally symmetrical current field of the ring (Figure 8).

4.3.1. *Swell.* In the swell case the significant wave height increases about 30% just beyond the counter-current area and it decreases about 30% just beyond the following-current area (Figure 9). In such a swell situation a ship may therefore encounter nearly a doubling of the significant wave height when traveling from south to north along the lee side of the ring. These variations are well understood from refraction and straining effects. Refraction induces convergence of wave propagation in and beyond the countercurrent region and divergence in and beyond the following current region. This is illustrated in Figure 8 with the ray pattern for a monochromatic wave of 14-s period (nearly the peak period of the swell considered here) propagating across the ring (provided by J. Dekker of Delft Hydraulics; other examples are given by *Mapp et al.* [1985], *Dobson and Irvine*, [1983], and *Mathiesen* [1987]). The region of ray convergence and divergence just downwave from the countercurrent and following current areas respectively correspond well with the regions of maximum and minimum significant wave height in the model results. *Dobson and Irvine* [1983] speculate that the amplification or reduction in wave height can easily be a factor of 2 or more. This is not borne out by our results for this swell case, where the amplifications and reductions are much smaller. The reason for this is most probably the random, short-crested nature of the waves which diffuses caustic-type effects, even in the case of swell (see our comments in section 2). *Mathiesen* [1987] considers random, short-crested waves without wind but with a relatively wide directional distribution crossing a whirl. He finds a reduction in significant wave height of 20% just downwave from the whirl and an amplification of 15%. Our results for such short-crested, random waves with the effects of wind added show an even smaller reduction and amplification (see the storm case below).

The mean wave direction varies only mildly across the ring (12° maximum) and it returns to nearly its undisturbed value at a few diameters' distance downwave from the ring (wave direction vectors are shown in Figure 9). These mild variations seem to contrast with the strong refraction effects in the wave ray pattern of Figure 8. Not only is the variation of the mean wave direction milder than the directional variation of individual rays, it is also not as long-lasting as the ray pattern suggests. The reason is that downwave from the areas of divergence and convergence, the refracted rays diverge so that the energy represented by these rays decreases and the undisturbed rays dominate. In other words, the divergence of the refracted rays dilutes any effect that they may have on the mean wave direction. In addition, downwave from the ring the short-crestedness of the incoming waves mixes disturbed and undisturbed wave components rapidly. This diffusing effect of directional dispersion is enhanced by the frequency dispersion of the waves. These three diluting effects are not evident in ray patterns of monochromatic waves. The interpretation of such patterns is therefore not trivial. It is even less so where it concerns the short-crestedness which varies considerably: σ_θ from about 20° maximum in the countercurrent region to about 8° in the following-current region (over a distance of only 60 km). At larger distances the short-crestedness is only mildly affected.

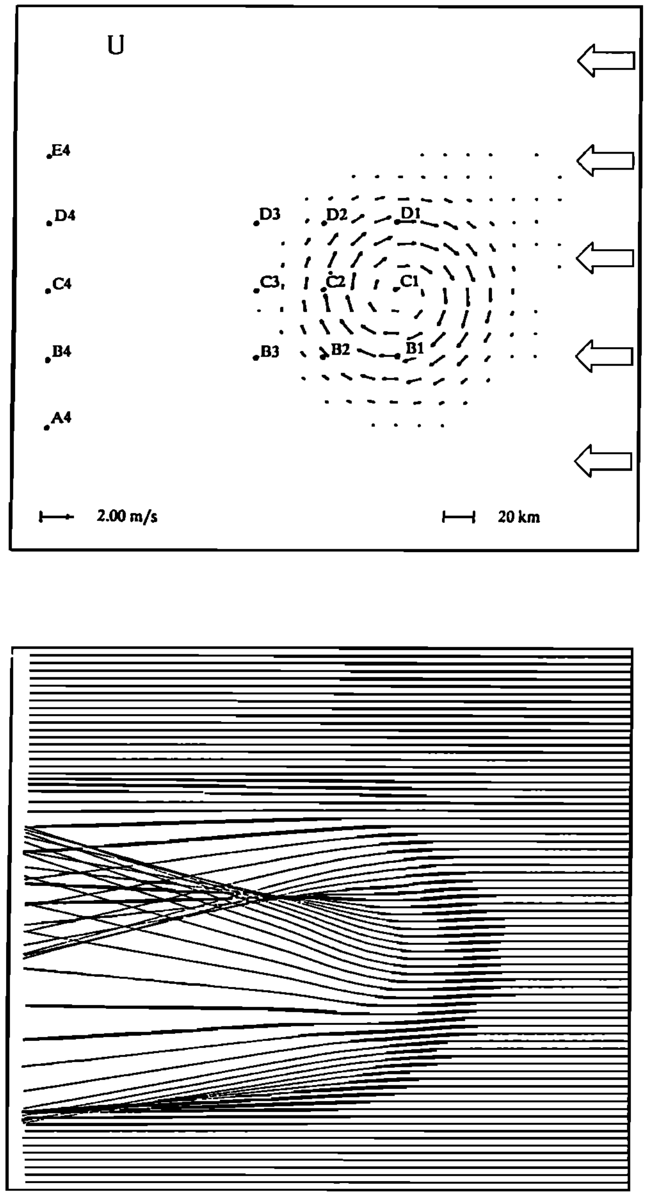

Fig. 8. Current field of the Gulf Steam ring with the locations of spectral information and the wave ray pattern for a 14-s-period wave. Wide arrows indicate incoming wave direction.

Upwave from the ring center the spectra are hardly

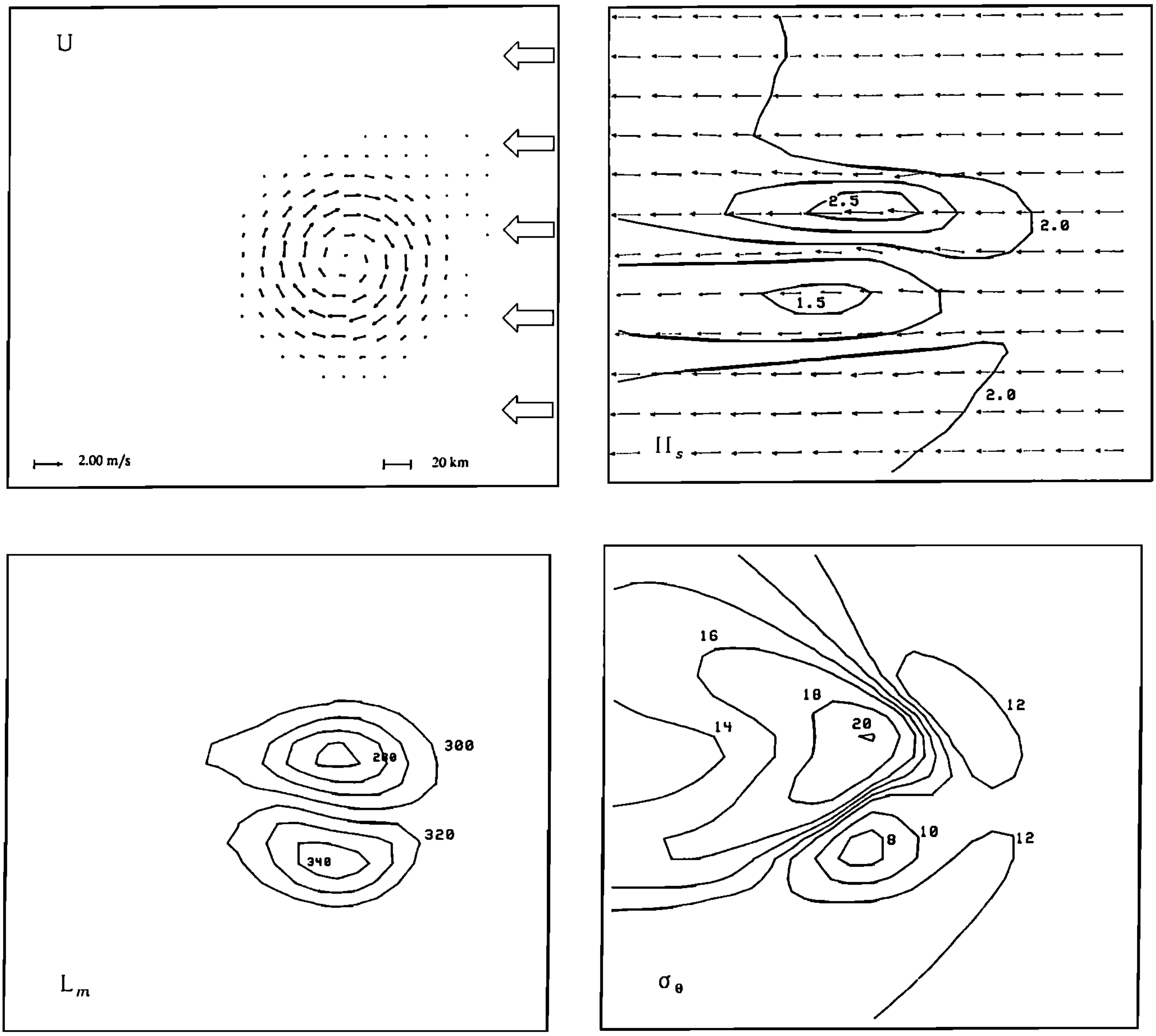

Fig. 9. Contour line plots in the ring area for swell: significant wave height (H_s in meters), mean wave length (L_m in meters) and directional spreading (σ_θ in degrees). Vectors indicate current or mean wave direction. Wide arrows indicate incoming wave direction.

affected (Figure 10, spectra B1, C1, and D1). Downwave from the ring center the spectra grow narrower over the following-current region (spectra B1, B2, and B3) and they grow wider over the countercurrent region (spectra D1, D2 and D3). An inspection of the wave ray pattern (Figure 8) indicates that this corresponds to the divergence and the convergence of rays in these regions. The spectra at some distance beyond the ring show that the long-distance refraction effect of the ring is to send some wave energy west-southwest and west-northwest. This is obvious from the secondary peaks in spectra B4 and E4 (Figure 10). The occurrence of these secondary peaks explains the larger values of the directional width at these locations (Figure 9). It is remarkable that the spectrum straight beyond the countercurrent region (spectrum D4) does not show such a bimodality (only a fairly wide and flat peak). *Mathiesen* [1987] finds a similar pattern of bimodality and unimodality in the directional spectra at the lee side of the whirl which he considers. However, his conclusion that the changes in the directional properties are considerable seems to refer to the shape of the directional spectrum rather than to the mean wave direction.

4.3.2. *Storm.* In the storm case the pattern of the significant wave height is fairly similar to that in the swell case but with some obvious differences (Figure 11). The location and extent of the perturbation of the wave field is more confined to the ring and the relative variations are smaller (but still considerable: from 10.1 m in the countercurrent region to 8.2 m in the following-current region). Both the mean wave direction and the short-crestedness vary only mildly across the ring, and they show no lasting effects beyond the ring.

Straining, convergence, and divergence of wave propagation again seem to be responsible for the enhancement and diminution of the significant wave height. The fact that this pattern is more confined to the ring area than in the swell

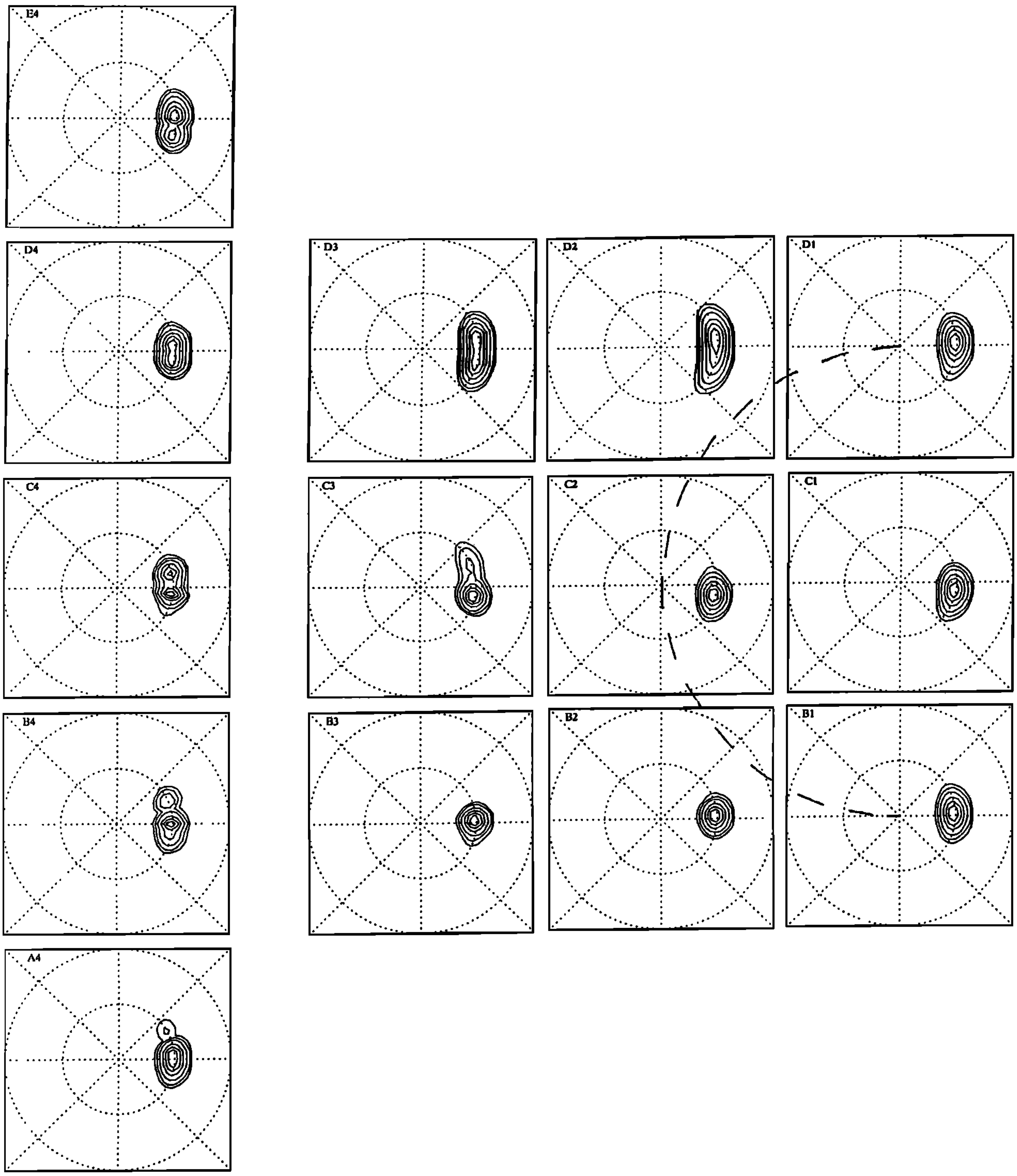

Fig. 10. Two-dimensional spectra for swell in the ring area at the labeled locations of Figure 8. The spectra are geographically arranged with spectrum C1 located at the center of the ring and spectra B1, C2 and D1 located at the radius to maximum current speed (indicated with dashed half circle). For plot legend, see Figure 2.

case is readily explained with the broader incoming spectrum (both in frequencies and directions) and the wind. The increased directional spreading diffuses the pattern laterally (increasingly in downwave direction), and the higher frequencies refract stronger than the swell, bringing the disturbed area closer to the ring, even if the peak frequency in the storm is nearly equal to the swell frequency. For the same reasons the variation in mean wave direction is milder than in the swell case. The occurrence of cross seas beyond the region of convergence is also suppressed by the broader spectrum (and probably the wind). This is obvious from the unimodal character of the directional spectra in the storm at locations where they are distinctly bimodal in the swell case (Figure 12).

Again, as in the storms in the straight Gulf Stream, the physical processes of wind generation, dissipation and nonlinear wave-wave interactions are considerably affected by the currents (Figure 13). The maximum enhancement of the

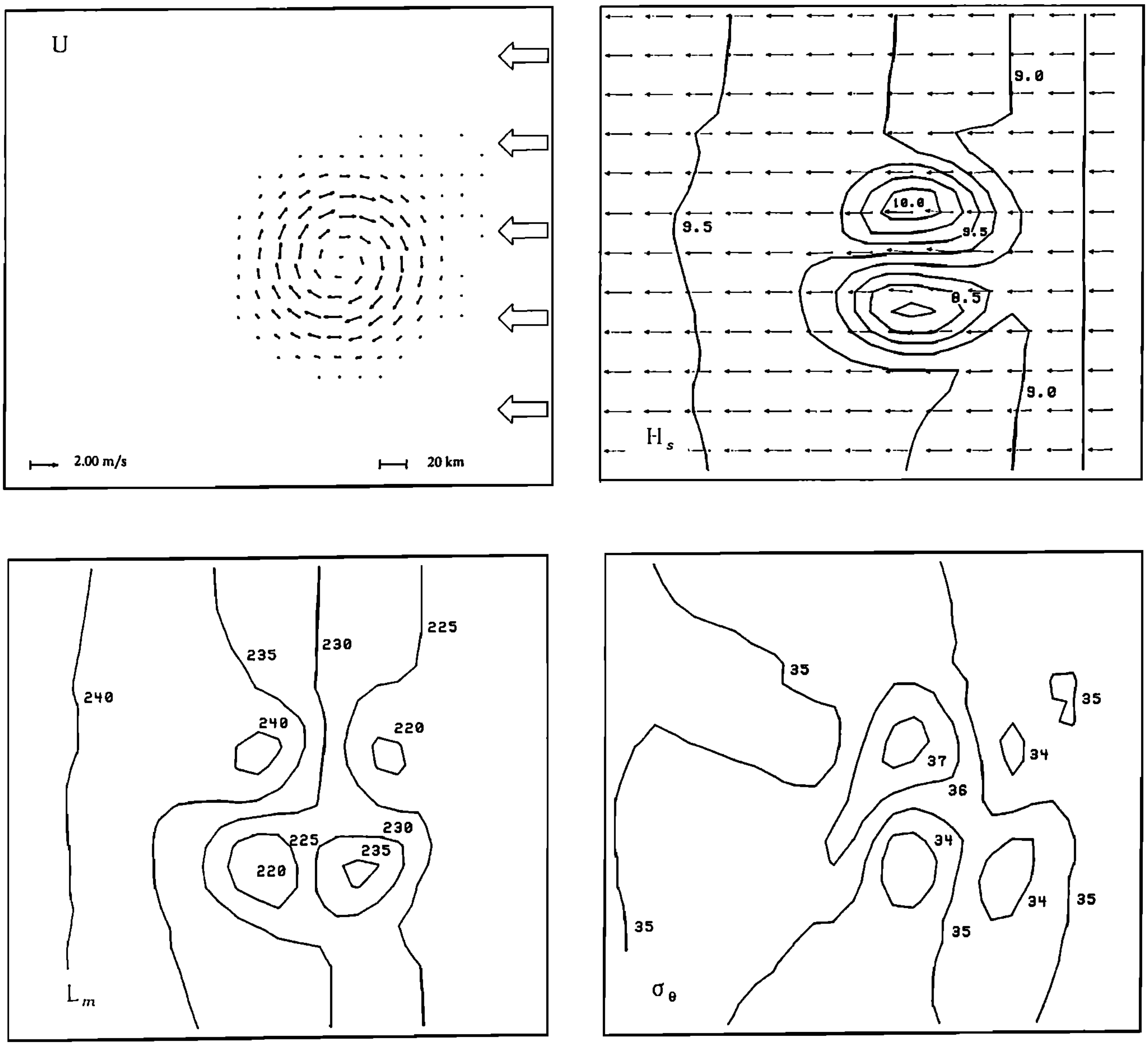

Fig. 11. Contour line plots in the ring area for storm conditions: significant wave height (H_s in meters), mean wave length (L_m in meters) and directional spreading (σ_θ in degrees). Vectors indicate current or mean wave direction. Wide arrows indicate incoming wave direction.

wind input is about 45% (near the maximum countercurrent, compared with the undisturbed situation, for instance, at the lateral boundaries of the model). The maximum enhancements of the dissipation and the nonlinear wave-wave interactions are about twice that value (in percent, i.e., ~90%). The maximum reductions are about half the maximum enhancements (opposite sign, in percent, i.e., ~20 and ~45%, respectively) for all three processes. These patterns, being almost identical with the pattern of the along-wave current component, suggests that these effects are locally induced by the currents, mostly through changing the wave steepness but probably also through a change in relative wind speed. The pattern of the processes show that the waves, after leaving the current field, slightly overshoot the undisturbed situation. We speculate that this may be due to a readjustment of the spectrum to different equilibrium levels (mostly at high frequencies). Figure 13 shows that the work done by the radiation stresses when the waves enter the ring is returned when they leave the ring. Again (as in the Gulf Stream storm cases), it is only a small fraction of the intensity of generation and dissipation each. However, at the location of maximum countercurrent its value is about 40% of the sum of wind input and dissipation. Ignoring the radiation stresses in a wave model would therefore affect the model results in the ring appreciably.

5. CONCLUSIONS

If waves from the open ocean travel across the straight Gulf Stream from an oblique direction, refraction is the dominating mechanism affecting the waves. Its most notable effect is the trapping of locally generated waves in an adverse-wind situation (wind against the current) and reflection of incoming waves if waves approach from a current-

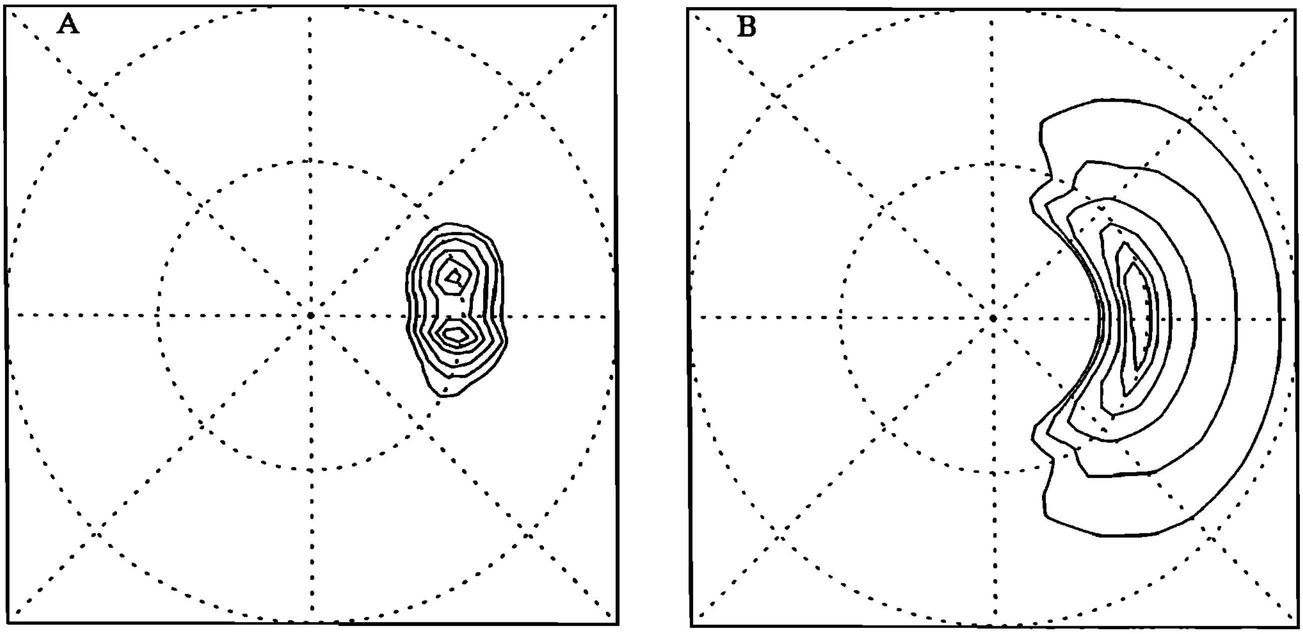

Fig. 12. Two-dimensional spectra for (*a*) swell conditions and (*b*) storm conditions at location C4 (see Figure 8). For plot legend, see Figure 2.

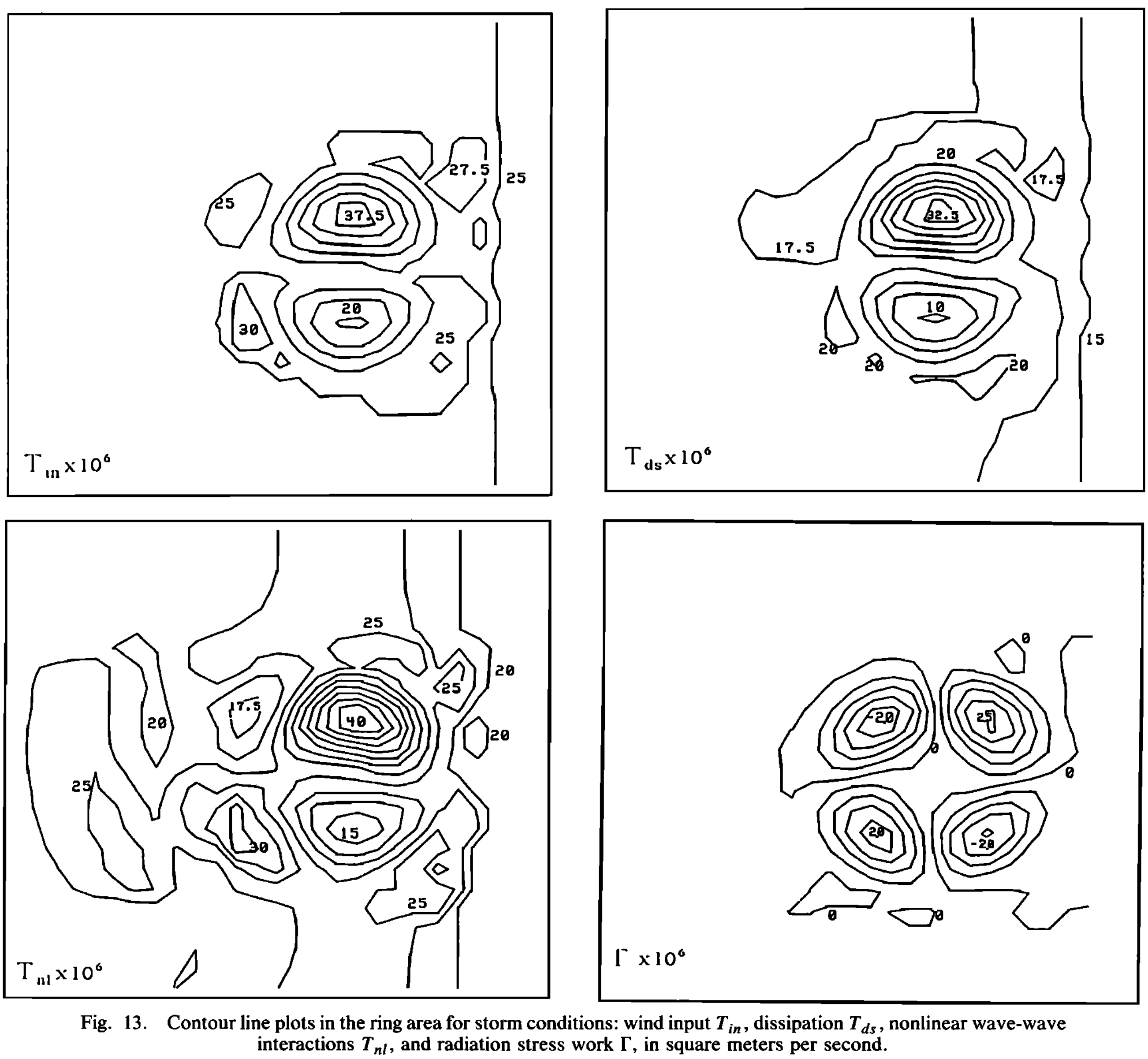

Fig. 13. Contour line plots in the ring area for storm conditions: wind input T_{in}, dissipation T_{ds}, nonlinear wave-wave interactions T_{nl}, and radiation stress work Γ, in square meters per second.

following direction. In a Gulf Stream ring, refraction considerably affects the significant wave height and the short-crestedness, but it affects the mean wave direction only slightly. Well-defined cross seas occur in a wide area beyond the ring in swell conditions but not in storm conditions. These effects are not as persistent as refraction computations for monochromatic, unidirectional waves suggest. In fact, they disappear after a few ring diameters as a result of the mixing of disturbed waves with undisturbed waves and the diluting effect of frequency and direction dispersion. Along the United States east coast the presence of the Gulf Stream will therefore be noticeable in the wave field only from an occasional reduction of incoming swell and from alongshore swell variations at the lee side of nearby rings (or meanders). In storms, practically no effects on the wave field along the coast will be noticeable. In offshore areas with currents, local effects can be considerable, partly because the processes of wave generation and dissipation are greatly affected there. The intensity of these processes is nearly doubled in countercurrent conditions and nearly halved in following current conditions (in the cases considered in this study). In particular, the large variation in whitecapping in Gulf Stream rings such as the one considered in this study should be noticeable in storm conditions. The work done by radiation stresses is not negligible compared with the overall effect of wave generation and dissipation.

Acknowledgements. With pleasure we acknowledge that the subject matter of this study was suggested by Mark Donelan of the Canada Centre for Inland Waters and Klaus Hasselmann of the Max Planck Institute for Meteorology in Hamburg. We sincerely thank Scott Glenn of Harvard University for providing the current fields and Johan Dekker of Delft Hydraulics for providing the wave ray pattern in the ring.

REFERENCES

Abbott, M. B., *Computational Hydraulics*, 324 pp., Pitman, London, 1979.

Beal, R. C., The Seasat SAR wind and ocean wave monitoring capabilities, *Rep. JHU/APL SIR79U-019*, 56 pp., Space Dep., Appl. Phys. Lab., Johns Hopkins Univ., Laurel, Md., 1980.

Booij, N., Gravity waves on water with non-uniform depth and current, Communications on Hydraulics, *Rep. 81-1*, 130 pp., Dep. of Civ. Eng., Delft Univ. of Technol., Delft, Netherlands, 1981.

Bretherton, F. P., and C. J. R. Garrett, Wave trains in inhomogeneous moving media, *Proc. R. Soc. London, Ser. A*, *302*, 529–554, 1968.

Christoffersen, J. B., Current depth refraction of dissipative water waves, *Ser. Pap. 30*, Inst. of Hydrodyn. and Hydraul. Eng., Tech. Univ. Denmark, Lyngby, 1982.

Dobson, E. B., and D. E. Irvine, Investigation of Gulf Stream ring detection with spaceborne altimeter using mean sea height, wave height and radar cross section, *Rep. JHU/APL S1R3U-005*, 51 pp., Space Dep., Appl. Phys. Lab., Johns Hopkins Univ., Laurel, Md., 1983.

Dorrestein, R., Simplified method of determining refraction coefficients for sea waves, *J. Geophys. Res.*, *65*(2), 637–642, 1960.

Fuglister, F. C., Cyclonic rings formed by the Gulf Stream, in *Studies in Physical Oceanography*, vol. I, pp. 137–168, Gordon and Breach, New York, 1971.

Glenn, S. G., A. R. Robinson, and M. A. Spall, Recent results of the Harvard Gulf Stream Forecasting Program, *Oceanogr. Mon. Summ.*, *7*(4), 3, 12–13, 1987.

Gutshabash, Ye. Sh., and I. V. Lavrenov, Swell transformation in the Cape Agulhas Current, *Izv. Acad. Sci. USSR Atmos. Oceanic Phys.*, Engl. Transl., *22*(6), 494–497, 1986.

Hasselmann, D. E., M. Dunckel, and J. A. Ewing, Directional wave spectra observed during JONSWAP 1973, *J. Phys. Oceanogr.*, *10*(8), 1264–1280, 1980.

Hasselmann, K., Grundgleichungen der Seegangsvoraussage, *Schiffstechnik*, *7*(39), 191–195, 1960.

Hasselmann, K., On the spectral dissipation of ocean waves due to white capping, *Boundary Layer Meteorol.*, *6*(1–2), 107–127, 1974.

Hasselmann, K., et al., Measurements of wind-wave growth and swell decay during the Joint North Sea Wave Project (JONSWAP), *Dsch. Hydrogr. Z.*, *8*(12), Suppl. A, 95 pp., 1973.

Hasselmann, S., et al. (WAMDI) Group), The WAM model—A third generation ocean wave prediction model, *J. Phys. Oceanogr.*, *18*(12), 1775–1810, 1988.

Hayes, J. G., Ocean current interaction study, *J. Geophys. Res.*, *85*(9), 5025–5031, 1980.

Hayes, R. M., Detection of the Gulf Stream, in *Spaceborne Synthetic Aperture Radar for Oceanography*, edited by R. C. Beal, P. S. DeLeonibus, and I. Katz, pp. 146–160, Johns Hopkins Press, Baltimore, Md., 1981.

Holthuijsen, L. H., N. Booij, and T. H. C. Herbers, A prediction model for stationary, short-crested waves in shallow water with ambient currents, *Coastal Eng.*, *13*, 23–54, 1989.

Huang, N. E., D. T. Chen, C.-C. Tung, and J. R. Smith, Interactions between steady non-uniform currents and gravity waves with applications for current measurements, *J. Phys. Oceanogr.*, *2*(4), 420–431, 1972.

Irvine, D. E., Extreme waves in the Agulhas—a case study of wave-current interaction, *Johns Hopkins APL Tech. Dig.*, *8*(1), 100–106, 1987.

Irvine, D. E., and D. G. Tilley, Ocean wave directional spectra and wave-current interaction in the Agulhas from the shuttle imaging radar–B synthetic aperture radar, *J. Geophys. Res.*, *93*(C12), 15,389–15,401, 1988.

Johnson, J. W., The refraction of surface waves by currents, *Eos Trans. AGU*, *28*(6), 867–874, 1947.

Jonsson, I. G., Wave-current interactions, in *The Sea*, vol. 9, *Ocean Engineering Science*, part A, edited by B. Le Méhauté and D. M. Hanes, pp. 65–120, John Wiley, New York, 1989.

Jonsson, I. G., and O. Skovgaard, Wave refraction across a shearing current, *Proc. Coastal Eng. Conf.*, *16th*, 722–741, 1978.

Kenyon, K. E., Wave refraction by currents, *Deep Sea Res.*, *18*, 1023–1034, 1971.

Komen, G. J., S. Hasselmann, and K. Hasselmann, On the existence of a fully developed wind-sea spectrum, *J. Phys. Oceanogr.*, *14*, 1271–1285, 1984.

Kuik, A. J., G. Ph. van Vledder, and L. H. Holthuijsen, A method for the routine analysis of pitch-and-roll buoy wave data, *J. Phys. Oceanogr.*, *18*(7), 1020–1034, 1988.

Lai, R. J., and S. L. Bales, Effects of the Gulf Stream on nearshore wave climate, *Proc. Coastal Eng. Conf.*, *20th*, 451–465, 1986.

Lavrenov, I. V., and V. V. Ryvkin, Evolution of average parameters of gravity waves in a current that varies along its propagation direction, *Izv. Acad. Sci. USSR Atmos. Oceanic Phys.*, Engl. Transl., *22*(10), 849–854, 1986.

Liu, A. K., F. C. Jackson, E. J. Walsh, and C. Y. Peng, A case study of wave-current interaction near an oceanic front, *J. Geophys. Res.*, *94*(C11), 16,189–16,200, 1989.

Longuet-Higgins, M. S., and R. W. Stewart, Changes in the form of short gravity waves on long waves and tidal currents, *J. Fluid Mech.*, *8*, 565–583, 1960.

Longuet-Higgins, M. S., and R. W. Stewart, The changes in amplitude of short gravity waves on steady non-uniform currents, *J. Fluid Mech.*, *10*, 529–549, 1961.

Longuet-Higgins, M. S., and R. W. Stewart, Radiation stress and mass transport in gravity waves, with application to "surf-beats," *J. Fluid Mech.*, *13*, 481–504, 1962.

Madsen, O. S., Y.-K. Poon, and H. C. Graber, Spectral wave attenuation by bottom friction: Theory, *Proc. Int. Coastal Eng. Conf.*, *21st*, 492–504, 1988.

Mapp, G. R., C. S. Welch, and J. C. Munday, Wave refraction by warm core rings, *J. Geophys. Res.*, *90*(C4), 7153–7162, 1985.

Mathiesen, M., Wave refraction by a current whirl, *J. Geophys. Res.*, *92*(C4), 3905–3912, 1987.

McClain, C. R., N. E. Huang, and P. E. LaViolette, Measurements of sea-state variations across oceanic fronts using laser profilometry, *J. Phys. Oceanogr.*, *12*(11), 1228–1244, 1982.

McKee, W. D., Waves on a shearing current: A uniformly valid asymptotic solution, *Proc. Cambridge Philos. Soc.*, *75*, 295–301, 1974.

McKee, W. D., A two turning-point problem in fluid mechanics, *Math Proc. Cambridge Philos. Soc.*, *77*, 581–590, 1975.

McKee, W. D., The reflection of water waves by shear currents, *Pure Appl. Geophys.*, *115*, 937–949, 1977.

McLeish, W., and D. B. Ross, Wave refraction in an ocean front, *J. Geophys. Res.*, *90*(C6), 11,929–11,938, 1985.

Meadows, G. A., R. A. Shuchman, Y. C. Tseng, and E. S. Kasischke, Seasat synthetic aperture radar observations of wave-current and wave-topographic interactions, *J. Geophys. Res.*, *88*(C7), 4393–4406, 1983.

Mei, C. C., *The Applied Dynamics of Ocean Surface Waves*, *Adv. Ser. Ocean Eng.*, vol. 1, 740 pp., World Scientific, Singapore, 1989.

Miles, J. W., On the generation of surface waves by shear flows, *J. Fluid Mech.*, *3*, 185–204, 1957.

Neu, W. L., and Y. S. Won, Propagation schemes for wind wave models with finite depth and current, in *Proceedings 11th International Annual Conference of the Canadian Applied Mathematics Society*, *Ocean Wave Mechanics*, *Computational Fluid Dynamics and Mathematical Modelling*, edited by M. Rahman, pp. 947–954, Computational Mechanics, Boston, Mass., 1990.

Peregrine, D. H., Interaction of water waves and currents, in *Advances in Applied Mechanics*, vol. 16, edited by C.-S. Yih, pp. 9–117, Academic, San Diego, Calif., 1976.

Phillips, O. M., On the generation of waves by turbulent wind, *J. Fluid Mech.*, *2*, 417–445, 1957.

Phillips, O. M., On the dynamics of unsteady gravity waves of finite amplitude, I, *J. Fluid Mech.*, *9*, 193–217, 1960.

Phillips, O. M., *The Dynamics of the Upper Ocean*, 2nd ed., 336 pp., Cambridge University Press, New York, 1977.

Pierson, W. J., Jr., and L. Moskowitz, A proposed spectral form for fully developed wind seas based on the similarity theory of S. A. Kitaigorodskii, *J. Geophys. Res.*, *69*(24), 5181–5190, 1964.

Robinson, A. R., M. A. Spall, and N. Pinardi, Gulf Stream simulation in the dynamics of ring and meander process, *J. Phys. Oceanogr.*, *18*(12), 1811–1853, 1988.

Sheres, D., K. E. Kenyon, R. L. Bernstein, and R. C. Beardsley, Large horizontal surface velocity shears in the ocean obtained from images of refracting swell and in situ moored current data, *J. Geophys. Res.*, *90*(C3), 4943–4950, 1985.

Smith, J., On surface gravity waves crossing weak current jets, *J. Fluid Mech.*, *134*, 277–299, 1983.

Smith, R., Giant waves, 3, *J. Fluid Mech.*, *77*, 417–431, 1976.

Snyder, R. L., F. W. Dobson, J. A. Elliott, and R. B. Long, Array measurements of atmospheric pressure fluctuations above surface gravity waves, *J. Fluid Mech.*, *102*, 1–59, 1981.

Sugimori, Y., Dispersion of the directional spectrum of short gravity waves in the Kuroshio current, *Deep Sea Res.*, *20*, 747–756, 1973.

Tolman, H. L., The numerical model WAVEWATCH: A third generation model for hindcasting of wind waves on tides in shelf seas, Communications on Hydraulic and Geotechnical Engineering, *Rep. 89-2*, 72 p., Fac. of Civ. Eng., Delft Univ. of Technol., Delft, Netherlands, 1989.

Tolman, H. L., Wind wave propagation in tidal seas, Communications on Hydraulic and Geotechnical Engineering, *Rep. 90-1*, 135 p., Fac. of Civ. Eng., Delft Univ. of Technol., Delft, Netherlands, 1990*a*.

Tolman, H. L., The influence of unsteady depths and tidal currents on wind-wave propagation in shelf seas, *J. Phys. Oceanogr.*, *20*(8), 1166–1174, 1990*b*.

Tolman, H. L., The influence of tides and storm surges on North Sea wind waves, *J. Phys. Oceanogr.*, *21*(6), 766–781, 1991*a*.

Tolman, H. L., A third generation model for wind waves on slowly varying, unsteady and inhomogeneous depths and currents, *J. Phys. Oceanogr.*, *21*(6), 782–799, 1991*b*.

Trulsen, G. N., K. B. Dysthe, and J. Trulsen, Evolution of a gravity wave spectrum through a current gradient, *J. Geophys. Res.*, *95*(C12), 22,141–22,151, 1990.

Tseng, Y. C., Wave-current and wave-topographic interactions using Seasat synthetic aperture radar observations and analytical ocean models, Ph.D. thesis, Univ. of Mich., Ann Arbor, 1985.

Whitham, G. B., A general approach to linear and nonlinear dispersive waves using a Lagrangian, *J. Fluid Mech.*, *22*, 273–283, 1965.

Willebrand, J., Energy transport in a nonlinear and inhomogeneous random gravity wave field, *J. Fluid Mech.*, *70*, 113–126, 1975.

L. H. Holthuijsen, Department of Civil Engineering, Delft University of Technology, Stevinweg 1, 2628 GA Delft, Netherlands.

H. L. Tolman, NASA Goddard Space Flight Center, Greenbelt, MD 20771.

(Received October 10, 1990;
revised March 26, 1991;
accepted March 26, 1991.)